

# DESIGNING RF PULSES WITH OPTIMAL SPECIFIC ABSORPTION RATE (SAR) CHARACTERISTICS AND EXPLORING EXCITATION FIDELITY, SAR AND PULSE DURATION TRADEOFFS

A. C. Zelinski<sup>1</sup>, V. K. Goyal<sup>1</sup>, L. Angelone<sup>2</sup>, G. Bonmassar<sup>2</sup>, L. L. Wald<sup>2,3</sup>, and E. Adalsteinsson<sup>1,3</sup>

<sup>1</sup>Department of Electrical Engineering and Computer Science, MIT, Cambridge, MA, United States, <sup>2</sup>MGH, Harvard Medical School, A. A. Martinos Center for Biomedical Imaging, Charlestown, MA, United States, <sup>3</sup>Harvard-MIT Division of Health Sciences and Technology, MIT, Cambridge, MA, United States

**INTRODUCTION:** Recent methods of designing RF pulses for multi-coil TX systems have focused on solving regularized systems of equations. These techniques linearize the equations relating the RF waveforms to the resulting excitation and then penalize RF candidates with high peak and root-mean-square (RMS) voltages ( $V_P$  and  $V_{RMS}$ , respectively) in an attempt to limit SAR [1,2]. This is sensible because in single-coil systems, SAR scales directly with  $V_P$  and  $V_{RMS}$ . In multi-channel systems, however, the simultaneous transmission of pulses through multiple coils causes their E-fields to interact, possibly adding constructively, which may significantly affect SAR. We account for these interactions in RF design techniques for multi-coil TX systems by explicitly optimizing SAR. This builds on Zhu's linear-algebraic formulation and optimization of SAR when designing RF pulses on  $P$ -channel TX systems [3], which requires knowledge of the steady state E-fields generated per unit of power sent to each TX coil, the tissue's electrical properties and spatial sensitivity profiles ( $B_1$  maps) of each coil. Then we pose optimization problems that produce RF pulses with optimal SAR characteristics. In particular, we provide a closed-form solution for optimizing mean SAR, introduce a method to explore excitation fidelity, mean SAR and pulse duration tradeoffs, pose a constrained optimization problem that ensures 10g average SAR meets certain constraints, and show that RF pulses generated by a mean SAR optimization algorithm have better properties than those produced via Tikhonov regularization.

**METHODS: Regularized RF pulse design.** For a  $P$ -channel TX system, linearizing and discretizing the equations relating the RF pulses played through each coil to the resultant excitation yields  $\mathbf{m}=\mathbf{A}\mathbf{b}_{full}$  [2,4], where  $\mathbf{m}$  is an  $M \times 1$  vector of the target excitation's samples in the region of interest and  $\mathbf{b}_{full}$  a  $PT \times 1$  voltage vector of samples of the RF waveforms containing  $T$  samples of each coil's RF pulse  $b_{1,p}(t)$ .  $\mathbf{A}$  is an  $M \times PT$  matrix incorporating each coil's  $B_1$  map and the fixed  $k$ -space trajectory. An example of a regularized RF design algorithm is a Tikhonov regularization:  $\min \|\mathbf{m}-\mathbf{A}\mathbf{b}_{full}\|_2 + \lambda \|\mathbf{b}_{full}\|_2$ , with  $\lambda$  penalizing high-energy  $\mathbf{b}_{full}$  candidates.

**Linear-algebraic formulation of SAR and design of RF pulses with optimal SAR characteristics.**

Analogously to Zhu [3], we derive a matrix-vector expression for  $s(r)$ , the SAR at spatial location  $r$ , defined as  $w(r) \sum_{t=1}^T \|\mathbf{E}(r,t)\|_2^2$ , where  $w(r)=\sigma(r)/(2\rho(r))^{-1}$ ,  $\sigma(r)$  and  $\rho(r)$  are the conductivity and mass density, respectively, and  $\mathbf{E}(r,t)$  is the complex-valued 3-D E-field at  $r$  at time  $t$  [5]. This E-field is a linear superposition of each TX coil's E-field, scaled by the RF playing along each:  $\mathbf{E}(r,t)=b_{1,1}(t)\mathbf{E}_1(r,t) + \dots + b_{1,P}(t)\mathbf{E}_P(r,t)$ , where  $b_{1,p}(t)$  is the RF played along the  $p$ th coil at  $t$  and  $\mathbf{E}_p(r,t)$  is a complex-valued 3-D vector of the E-field at location  $r$  and time  $t$  generated by the  $p$ th coil. This may be written compactly as follows:  $\mathbf{E}(r,t) = \mathbf{F}(r,t)\mathbf{b}_1(t)$ , where  $\mathbf{F}(r,t)=[\mathbf{E}_1(r,t), \dots, \mathbf{E}_P(r,t)]$  and  $\mathbf{b}_1(t)=[b_{1,1}(t), \dots, b_{1,P}(t)]^T$ . Substituting this into  $s(r)$  yields:

$$s(r) = w(r) \sum_{t=1}^T \mathbf{E}^H(r,t)\mathbf{E}(r,t) = w(r) \sum_{t=1}^T \mathbf{b}_1^H(t)\mathbf{F}^H(r,t)\mathbf{F}(r,t)\mathbf{b}_1(t) = w(r)\mathbf{b}^H\mathbf{G}(r)\mathbf{b},$$

where  $\mathbf{b}=[b_{1,1}(1), \dots, b_{1,P}(T)]^H$  ( $\mathbf{b}$  is simply a permutation  $\mathbf{Z}$  of  $\mathbf{b}_{full}$ ) and  $\mathbf{G}(r) = \text{diag}(\mathbf{F}^H(r,1)\mathbf{F}(r,1), \dots, \mathbf{F}^H(r,T)\mathbf{F}(r,T))$ . The block-diagonal  $\mathbf{G}(r)$  describes the E-fields over time at location  $r$  and  $s(r)$  is quadratic in  $\mathbf{b}$ . Now we form a vector of SAR at  $R$  points in the region of interest:  $\mathbf{s} = [s(r_1), \dots, s(r_R)]^T$ .

$$\mathbf{s} = \mathbf{W}[\mathbf{b}^H\mathbf{G}(r_1)\mathbf{b}, \dots, \mathbf{b}^H\mathbf{G}(r_R)\mathbf{b}]^T = \mathbf{W}(\mathbf{I}_R \otimes \mathbf{b}^H)[\mathbf{G}^H(r_1), \dots, \mathbf{G}^H(r_R)]\mathbf{b},$$

where  $\mathbf{W}=\text{diag}(w(r_1), \dots, w(r_R))$ ,  $\mathbf{I}_R$  is the  $R \times R$  identity matrix and  $\otimes$  is the Kronecker product. Because the  $\mathbf{G}(r_i)$ ,  $\mathbf{W}$  and  $T$  are known, SAR at each point depends only on  $\mathbf{b}$ . Note: we assume no coupling between coils; cross-terms must be added if coupling is indeed present. Now that we have a tractable expression for  $\mathbf{s}$ , and recalling the  $\mathbf{m}=\mathbf{A}\mathbf{b}_{full}=\mathbf{A}\mathbf{Z}\mathbf{b}=\mathbf{F}\mathbf{b}$  system of equations [2,4], we may now solve any optimization that explicitly constrains or regularizes SAR, e.g.,  $\min_{\mathbf{b}} \|\mathbf{m}-\mathbf{F}\mathbf{b}\|_2$  s.t.  $\|\mathbf{s}\|_{\infty} \leq M$ .

**Closed-form solution for mean-SAR optimization.** We explore optimally minimizing the residual error (i.e., maximizing the excitation fidelity) while limiting the mean SAR. First, we compute the mean SAR by analyzing  $\mathbf{E}[\mathbf{s}] = R^{-1}(s(r_1) + \dots + s(r_R)) = R^{-1}[w(r_1)\mathbf{b}^H\mathbf{G}(r_1)\mathbf{b} + \dots + w(r_R)\mathbf{b}^H\mathbf{G}(r_R)\mathbf{b}] = \mathbf{b}^H\mathbf{Q}\mathbf{b}$ , which shows  $\mathbf{E}[\mathbf{s}]$  is quadratic in  $\mathbf{b}$ , in agreement with [3]. Whereas Zhu solves the following constrained optimization:  $\min_{\mathbf{b}} \mathbf{b}^H\mathbf{Q}\mathbf{b}$  s.t.  $\mathbf{m}=\mathbf{F}\mathbf{b}$  [3], we minimize mean SAR in a different manner by relaxing the linear constraint  $\mathbf{m}=\mathbf{F}\mathbf{b}$  and introducing a Lagrange multiplier. Defining the cost function  $J(\mathbf{b}) = \|\mathbf{m}-\mathbf{F}\mathbf{b}\|_2^2 + \lambda \mathbf{E}[\mathbf{s}(\mathbf{b})] = \|\mathbf{m}-\mathbf{F}\mathbf{b}\|_2^2 + \lambda \mathbf{b}^H\mathbf{Q}\mathbf{b}$ , one may show that  $\mathbf{b}^* = [\mathbf{F}^H\mathbf{F} + \lambda\mathbf{Q}]^{-1}\mathbf{F}^H\mathbf{m}$  is the optimal closed-form solution that minimizes  $J(\mathbf{b})$ . Since  $\mathbf{Q}$ ,  $\mathbf{F}$  and  $\mathbf{m}$  are known, this optimal solution  $\mathbf{b}^*$  is simply a function of  $\lambda$ . When  $\lambda$  is fixed,  $\mathbf{b}^*$  may be rapidly computed by solving  $[\mathbf{F}^H\mathbf{F} + \lambda\mathbf{Q}]\mathbf{b} = \mathbf{F}^H\mathbf{m}$  via a conjugate-gradient method. After solving for  $\mathbf{b}^*$ , it may be substituted back into the mean SAR and residual error equations, reducing them to functions of  $\lambda$  as well.

**Exploring excitation fidelity, SAR and pulse duration tradeoffs.** Solving the system above for many values of  $\lambda \in [0, \infty)$  generates a curve of the lowest residual error  $\|\mathbf{m}-\mathbf{F}\mathbf{b}\|_2$  achievable vs.  $\mu_{SAR}$ . This allows one to explore the entire range of fidelity-SAR tradeoffs. One may extend this concept by allowing  $T$  to vary as well, i.e., turning the number of pulse samples (and hence overall pulse duration) into a free variable. Then solving the system of equations for many  $(T, \lambda)$  pairs generates a contour of the best residual error achievable for a given  $\mu_{SAR}$  and pulse duration, illuminating fidelity vs.  $\mu_{SAR}$  vs. pulse duration tradeoffs.

**10g SAR optimization.** We now pose a constrained optimization that provides the highest-fidelity excitation while ensuring  $N$  total 10g SAR averages meet fixed constraints:  $\min_{\mathbf{b}} \|\mathbf{m}-\mathbf{F}\mathbf{b}\|_2$  s.t.  $\mathbf{b}^H\mathbf{Q}_n\mathbf{b} \leq M_1, \dots, \mathbf{b}^H\mathbf{Q}_N\mathbf{b} \leq M_N$ , where  $\mathbf{Q}_n = \Sigma_i \mathbf{G}(r_i)$ ,  $\forall i \in I_n$ , and  $I_n$  is an index set into the  $\{r_i\}$  designating 10g of tissue, i.e.,  $\Sigma_i \rho(r_i) = 10\text{g}$ .

**E-field calculations.** Steady-state E-fields in one slice of a 29-tissue, high-resolution ( $1 \times 1 \times 2 \text{mm}^3$ ) anatomically-accurate segmented head model are computed via finite difference time domain simulations of an 8-channel system at 7T [6], yielding  $\mathbf{E}_p(r,t)$  for each of the  $P=8$  coils. There are  $\sim 30\text{k}$  pixels in the region of interest, so  $R=30\text{k}$ . The system and a slice of the head model are illustrated in Fig. 1. Since tissue properties are present in the model, each of the  $\mathbf{G}(r_i)$  and  $\mathbf{Q}$  are computable.

**RESULTS:** We fix the  $k$ -space trajectory to be a 2-D spiral with an acceleration factor of 4 and the target to be an MIT logo.  $B_1$  maps from an 8-coil system are known [7], so  $\mathbf{m}$  and  $\mathbf{A}$  are implicitly defined. The RF waveforms are uniformly sampled with  $\Delta t=5\mu\text{s}$  and  $T=484$ , so the duration of each RF pulse is  $\sim 2.4$  ms. In Fig. 2, optimal residual error vs. mean SAR tradeoffs are explored. To prove that the mean-SAR optimization method outperforms standard regularized-pulse designs, we design a Tikhonov-regularized RF pulse set (using the LSQR algorithm [8,9]) and a mean-SAR optimized set, tuning the parameters of each method such that the resulting pulses yield equal-fidelity excitations. Fig. 3 compares the voltage and SAR of the pulses generated by each method. Even though the Tikhonov-regularized pulses have lower  $V_{RMS}$ , they generate 1.29x higher  $\mu_{SAR}$ , which reinforces our claim that E-field interactions in parallel TX systems significantly influence SAR.

**ACKNOWLEDGEMENTS & REFERENCES:** NIH P41RR14075, US DoD NDSEG Fellowship, R. J. Shillman Career Dev Award. [1] Yip et al. Iterative RF pulse design for multidimensional, small-tip angle selective excit. *MRM*. 2005;54(4):908-917. [2] Grissom et al. Spatial Domain Method for the Design of RF Pulses in Multicoil Parallel Excit. *MRM*. 2006;56(3):620-629. [3] Zhu. Parallel Excit with an Array of Trans Coils. 2006;51:775-784. [4] Grissom et al. A new method for the design of RF pulses in Trans SENSE. *2nd Int'l Workshop on Parallel Imaging*, 2004; 95. [5] Katscher et al. Parallel RF trans. in MRI. *NMR Biomed*, 2006;19:393-400. [6] Angelone et al. Effect of TX array phase relationship on SAR. *ISMRM* 2006. [7] Setsompop et al. Parallel RF Trans with 8 Chan at 3T. *MRM*. 2006;56(5):1163-1171. [8] Paige et al. LSQR: An algorithm for sparse linear eqns and sparse least squares. *ACM Trans. Math. Soft.*, 1982;8(1):43-71. [9] Zelinski et al. RF Pulse Design Methods for Reduc of Image Artifacts in Parallel RF Excit. *ISMRM* 2007.

Fig 1: (a) 8-Coil Sys. (b) Head Model

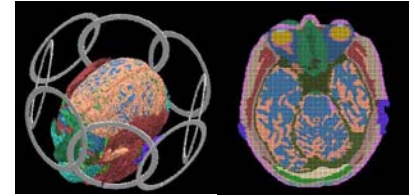


Fig 2: Optimal Mean SAR vs. Excit. Fidelity

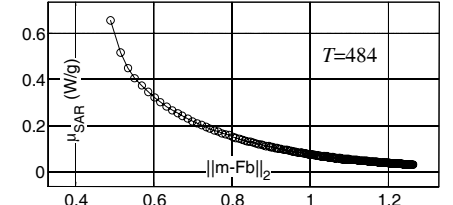


Fig 3: Tikhonov vs. Optimal SAR RF Design

